Sequential separation and profiling of extracellular vesicles using antibody-aptamer conjugates

D. Brambilla[1]*, F. Panico[1], M. S. Ünlü[2], M. Chiari[1].

[1] *National Research Council of Italy, Institute of Chemical Sciences and Technology (CNR-SCITEC), via Mario Bianco 9, 20131, Milan, Italy.*

[2] *Boston University, Electrical and Computer Engineering Department, 8 Saint Mary's St., Boston, MA, 02215, USA.*

** corresponding author: dario.brambilla@scitec.cnr.it*

Abtract

Extracellular vesicles (EVs) are membrane-bound vesicles secreted by cells, exhibiting diverse compositions reflective of their cellular origin. With significant potential as biomarkers for liquid biopsies, EV research has led to various isolation techniques. However, a consensus on the optimal strategy remains elusive. Immunoprecipitation, selectively capturing EVs based on surface markers, is promising but hindered by cost, low yields, and potential damage during release. In this study, we propose an innovative Antibody-Aptamer Conjugate: a three-component separation reagent for the separation of EVs. Combining an EV-specific antibody, a streptavidin-binding aptamer, and a unique barcode DNA sequence, this conjugate serves dual roles, facilitating both EV separation and subsequent multiplexed analysis.

We detail the development and validation of the Antibody-Aptamer Conjugate, demonstrating its efficacy in isolating intact EVs from complex samples. The unique barcode DNA sequence enables high-throughput analysis on a DNA microarray chip, addressing limitations of existing methodologies. This approach offers a valid and cost-effective alternative for selective EV isolation and analysis, with implications for diagnostic and therapeutic advancements in liquid biopsy applications.

1. Introduction

Extracellular vesicles are membranous vesicles secreted by cells into bodily fluids in both physiological and pathological conditions [1,2]. Their composition is intricately linked to the nature and condition of the originating cell, encompassing both their membrane structure

and cargo content. Consequently, EVs have garnered significant interest as prospective biomarkers for liquid biopsies, prompting advancements in the research pertaining to the isolation and characterization of EVs [3,4].

Despite the ever-growing body of research dedicated to EVs, an unanimous consensus has yet to be reached regarding the selection of an optimal strategy for their separation. Presently, a variety of techniques are at disposal, such as ultracentrifugation, ultrafiltration, polymer-induced precipitation, immunoprecipitation, and microfluidics. Regrettably, each of these techniques is not devoid of limitations, and the choice of the most appropriate method (or combination of methods) must be made on a case-by-case basis, taking into account the specific demands of the experiment [5–11].

In the context of liquid biopsy applications, where the precise selection of specific and often sparsely represented subpopulations of extracellular vesicles (EVs) is essential to detect disease-related vesicles amidst a substantial excess of contaminants [12,13], the most promising separation approach is immunoprecipitation. This technique effectively utilizes antibodies as capture agents to selectively isolate EV subpopulations based on their membrane composition, provided that distinct surface markers are available.

Unfortunately, immunoprecipitation methods come with several limitations, such as the high cost of antibodies, low recovery yields, and the challenging release of EVs from the antibody. While cost may not pose a significant hurdle in diagnostic applications, other factors indeed impede the use of immunoprecipitation as a separation strategy for EVs. In particular, the release of EVs from the antibodies involves steps that often entail harsh conditions known to potentially damage the integrity of EVs, thereby compromising their analysis through imaging techniques (e.g., Nanoparticle Tracking Analysis, Transmission Electron Microscopy, AFM measurements) [14]. To date, only a few research groups have succeeded in developing immunoprecipitation methodologies capable of releasing intact EVs [15–17].

In this study, we propose an innovative approach centered around a three-component separation reagent (also called Antibody-Aptamer Conjugate throughout the text) that serves dual purposes, facilitating both EV separation and analysis. More specifically, as depicted in Figure 1, this reagent is a conjugate consisting of: i) an antibody that targets extracellular vesicles' surface markers; ii) a streptavidin-binding aptamer responsible for immobilizing the capture agent onto streptavidin-coated beads [18]; and iii) a unique barcode DNA sequence enabling the multiplexed analysis of isolated EVs on a DNA microarray chip.

2. Materials & Methods

2.1 Materials

Ammonium sulfate ($(NH_4)_2SO_4$), phosphate buffer saline tablets (PBS), Trizma base, 37% chloric acid (HCl), sodium phosphate (Na_3PO_4), sucrose monolaurate, sodium chloride (NaCl), ethanolamine, trehalose dehydrate, magnesium chloride ($MgCl_2$), sodium azide (NaN_3), streptavidin, Dibenzocyclooctyne-N-hydroxysuccinimyde ester (DBCO-NHS ester), Amicon Ultra 100MWCO centrifugal filters and polyclonal rabbit IgG were purchased from Sigma Aldrich (St. Louis, MO, USA). Mouse anti-human CD9 IgG (clone MEM-61) and biotinylated mouse anti-human CD9 IgG (clone MEM-61) were a kind gift of Hansa BioMed Life Sciences Ltd (Tallinn, Estonia). Cy3-labeled goat antirabbit IgG was purchased from Jackson ImmunoResearch (Baltimore, PA, USA). Oligonucleotides were synthesized by MWG-Biotech AG (Ebevsberg, Germany). Oligonucleotides were modified in 5' position with either a C6 amino-linker and a C3 azido-linker. Oligonucleotides were freeze-dried and resuspended in de-ionized water (DI water) at a final concentration of 100 µM before use. Dynabeads M-270 Streptavidin magnetic beads were purchased from Thermofisher (Waltham, MA, USA). Untreated silicon chips with 100 nm thermal grown oxide (14 x 14 mm) were supplied by SVM, Silicon Valley Microelectronics Inc. (Santa Clara, CA, USA). NV10B silicon chips were supplied by NanoView Biosciences (Boston, MA, USA). Both chips were pretreated using a HARRICK Plasma Cleaner, PDC-002 (Ithaca, NY, USA), connected to an oxygen line. MCP-2 was purchased from Lucidant Polymers Inc. (Sunnyvale, CA, USA). Spotting is performed using SciFLEXARRAYER S12 (Scienion, Berlin, Germany). Fluorescence images were obtained using the ScanArray Lite confocal laser scanner and analyzed using ScanArray Express software (Perkin Elmer, MA, USA). Interferometric and fluorescence analyses of EVs were performed exploiting SP-IRIS technique using ExoView™ R100 for image acquisition and nanoViewer 2.6.0 software for analysis (NanoView Biosciences Inc., MA, USA). This instrument measures the number of single particles (ranging from 50 to 200 nm in diameter) captured on the chip surface as well as their size distribution. Nanoparticle Tracking Analysis was performed with NanoSight NS300 using 3.2 Dev Build 3.2.16 software (Malvern Instruments Ltd, Malvern, United Kingdom). Antibody Aptamer Conjugates were purified using proFIRE instrument (Dynamic Biosensors GmbH, Munchen, Germany). Western Blot analyses were performed using JESS Simple Western (Bio-Techne, Minneapolis, MN, USA).

2.2 Synthesis of AACs: Antibody-Aptamer Conjugates (general procedure)

The following procedure has been adapted starting from [19]. To a sodium azide free antibody solution (100 µL, 1 mg/mL) 2.46 µL of DBCO-NHS ester 4 mM (15 equivalents) were added and the mixture was allowed to react 30 min at room temperature. The reaction was quenched in 5 min at room temperature by adding 10 µL of 1 M Tris/HCl pH 8.0. Unreacted DBCO-NHS ester was removed through centrifugation on Amicon Ultra 100 MWCO filters (3 × 5 min at 12.000×*g*). After centrifugation, DNA-antibody conjugation was performed by adding 27 µL (4 equivalents) of azido-modified DNA from a 100 µM stock solution to 100 µL of DBCO-modified antibody. The reaction mixture was incubated overnight at 37 °C. Purification of the AAC was made using proFIRE instrument, and the AAC-containing fractions were concentrated and buffer exchanged to PBS-M on an Amicon Ultra 100 MWCO filters using multiple centrifugation steps at 12.000x*g*). Final conjugate concentrate was measured using Nanodrop Lite (Thermo Fisher Scientific, Waltham, MA, USA).

2.3 Oligonucleotide sequences

Different ssDNA sequences were used within this work:

- ***StrepApt5****: 5'-GGGAACGCACCGATCGCAGGTTTCCC-3'*
- ***StrepApt5-5A****: 5'-AAAAAGGGAACGCACCGATCGCAGGTTTCCC-3'*
- ***Tag1****: 5'-AAAAAGGGAACGCACCGATCGCAGGTTTCCCATCGTACTTGGCACTGGAGT-3'*
- ***Tag2****: 5'-AAAAAGGGAACGCACCGATCGCAGGTTTCCCCCGCGACCAGAATTAGATTA-3'*
- ***Tag3****: 5'-AAAAAGGGAACGCACCGATCGCAGGTTTCCCGCCCAAATAAGACGTGAGCC-3'*
- ***Probe1****: 5'-AAAAAAAAAAAAAAAAAAAAACTCCAGTGCCAAGTACGAT-3'*
- ***Probe2****: 5'-AAAAAAAAAAAAAAAAAAAATAATCTAATTCTGGTCGCGG-3'*
- ***Probe3****: 5'-AAAAAAAAAAAAAAAAAAAAGGCTCACGTCTTATTTGGGC-3'*
- ***Stabilizer****: 5'-TTTTTTTTTTTTTTTTTTT-3'*

DNA sequences used to be conjugated to mammalian IgGs were modified at 5' end with an azide group and used as described in Section 2.2. Probe sequences were modified at 5' end with an amino group in order to be immobilized on microarray chips as described in Section 2.4. Stabilizer sequence was used without any modification.

2.4 Functionalization of microarray chips (general procedure)

Silicon supports were pretreated with oxygen plasma to clean and activate the surface. The oxygen pressure was set to 1.2 bar with a power of 29.6 W for 10 min. Then chips were dipped into a 1% w/v solution of MCP-2 in 0,9M aqueous ammonium sulfate. The supports

were immersed into the coating solution for 30 min at room temperature, rinsed with bidistilled water, dried under nitrogen stream and then cured at 80 °C for 15 min.

Supports were spotted using a noncontact microarray spotter (sciFLEXARRAYER S12, Scienion, Berlin) equipped with an 80 µm nozzle. 400 pL of solution were spotted at room temperature and 65% humidity.

To prepare spotting solutions proteins were dissolved in PBS or PBS containing 50 mM trehalose, while oligonucleotides were dissolved in a solution of 150 mM sodium phosphate buffer containing 0.01% sucrose monolaurate at pH 8.5. After spotting chips were stored overnight in a sealed chamber filled at the bottom with sodium chloride saturated water (40 g/100 mL H_2O, 65% humidity). Finally, chips were treated with a blocking solution of ethanolamine (50 mM in 0.1M Tris/HCl buffer pH 9 and 2 mM $MgCl_2$) at room temperature for 1 h, rinsed with bidistilled water and dried.

2.5 Functionalization of magnetic beads coated with streptavidin (general procedure)

0.5 mg of streptavidin coated magnetic beads were washed twice with 100 µL of PBS-M. Beads were then incubated with 100 µL of 30 µg/mL AAC in PBS-M for 1 h at 25°C under stirring. After incubation the supernatant was removed and beads were washed twice with 100 µL of PBS-M and used for following experiments.

2.6 Capture and release of AACs on microarray chips

Twelve silicon chips were coated using MCP-2 and spotted with different concentrations of streptavidin in PBS (namely 0.2, 0.5, 1 and 2 mg/mL) as described in Section 2.4. Six chips were incubated with 30 µg/mL Rabbit IgG-StrepApt5 conjugate in PBS-M for 1 h at RT, while remaining chips were incubated under the same experimental conditions using 30 µg/mL Rabbit IgG-StrepApt5-5A in PBS-M. Chips were washed 10 min with PBS-M, rinsed with 2 mM $MgCl_2$ and dried under nitrogen stream. Then, half of the chips were incubated using 4 mM biotin in PBS for 1 h at RT and 80 rpm, washed 10 min with PBS-M, rinsed with 2 mM $MgCl_2$ and dried under nitrogen stream. All chips were then incubated with 10 µg/mL Cy3-labeled goat antirabbit IgG in PBS-M for 45 min at RT, washed 10 min in PBS-M, rinsed with 2 mM $MgCl_2$ and dried under nitrogen stream. Finally, chips were scanned using 65% laser power and 65% PMT.

The same experimental protocol was repeated on 18 silicon chips and used to test the capture and release efficiency for AACs obtained by the conjugation of Rabbit IgG with Tag1, Tag2 and Tag3.

2.7 Recapture of AACs on DNA microarray chips

Three aliquots of 0.5 mg of streptavidin coated magnetic beads, functionalized using Rabbit IgG-Tag1, Rabbit IgG-Tag2 or Rabbit IgG-Tag3 as described in Section 2.5, were incubated with 100 µL of 4 mM biotin in PBS for 1 h at 25°C under stirring. After incubation, supernatant was recollected and used to incubate six silicon chips (three chips for each AAC) coated with MCP-2 and spotted with RADI-Probe1, RADI-Probe2, and RADI-Probe3 (all probes were diluted to 25 µM and added with Stabilizer 25 µM in printing buffer) for 1 h at RT. Chips were then washed 10 min with PBS, rinsed with 2 mM $MgCl_2$ and dried under nitrogen stream. Chips were then incubated with 10 µg/mL Cy3-labeled goat antiRabbit IgG in PBS for 45 min at RT, washed 10 min in PBS, rinsed with 2 mM $MgCl_2$ and dried under nitrogen stream. Chips were scanned using 65% laser power and 65% PMT.

2.8 Separation of EVs from HEK-293 cell culture medium by ultracentrifugation

HEK-293 cells were seeded on 150 mm dishes in DMEM culture medium supplemented with 10% EV-depleted FCS (obtained by recovering the supernatant after ultracentrifugation of the FCS at 150.000 x g for 17 h), 2 mM L-Glutamine, 100 U/mL penicillin and 100 µg/mL streptomycin-sulphate. After 72 h incubation, the culture medium was collected and centrifuged (1500 rpm) for 25 min to remove cell debris. The obtained supernatant was filtered through 0.22 µm filter and then ultracentrifuged at 150.000 x g for 2 hours at 4° C (Beckman Coulter). The EV containing pellet was resuspended in PBS and their concentration was assessed using Nanosight NS300.

2.9 Reversible immune-capturing of HEK-derived EVs and recapture on DNA microarray

Two aliquots of 0.5 mg of streptavidin coated magnetic beads were functionalized with antiCD9-Tag2 as described in Section 2.5. One aliquot was then incubated with 200 µL of EVs ($1*10^{10}$ particles/mL in PBS-M, purified via ultracentrifugation as described in Section 2.8) for 2.5 h at 25°C under stirring. Beads were then washed twice with 100 µL of PBS-M and incubated with 100 µL of 4 mM biotin in PBS for 1 h at 25°C under stirring. As negative control, the second aliquot of beads was incubated with PBS-M instead of EVs following the same experimental protocol.

Six silicon chips were coated with MCP-2 and functionalized with Probe2, Probe3 and Rabbit IgG as described is Section 2.4. Supernatants recollected from beads were used to incubate

silicon chips (3 chips for each supernatant) for 1 h at RT. Chips were then washed 10 min in PBS rinsed with 2 mM $MgCl_2$ and dried. Chips were finally scanned using ExoView R100.

2.10 Plasma Samples

Pooled Human Plasma with sodium citrate as anticoagulant was purchased from Innovative Research (IPLAWBNAC50ML). Plasma was aliquoted and stored at -20°C.

2.11 Reversible immune-capturing of EVs from plasma and recapture on DNA microarray

0.5 mg of streptavidin coated magnetic beads were functionalized with antiCD9-Tag2 as described in Section 2.5. Beads were then incubated with 200 µL of human plasma added with 2 mM $MgCl_2$ for 2.5 h at 25°C under stirring. Beads were then washed twice with 100 µL of PBS-M and incubated with 100 µL of 4 mM biotin in PBS for 1 h at 25°C under stirring. Fifteen silicon chips were coated with MCP-2 and functionalized with Probe2, Probe3 and Rabbit IgG as described is Section 2.4. Supernatant recollected from beads were used to incubate three silicon chips for 1 h at RT. Chips were then washed 10 min in PBS rinsed with 2 mM $MgCl_2$ and dried. Chips were then incubated with Cy5-labeled antiCD63 and Cy3-labeled antiCD81 (each 1 µg/mL in PBS) for 45 min at RT. Chips were washed 10 min in PBS rinsed with 2 mM $MgCl_2$, dried and finally scanned using ExoView R100.

Two different aliquots of beads (0.5 mg each) were used as negative controls: the first one was functionalized with Rabbit IgG-Tag2 as described in Section 2.5, while the second was used without further modification. Then, aliquots were treated as described for beads functionalized with antiCD9-Tag2.

One additional negative controls was carried out: antiCD9-Tag2 was added to human plasma added with 2 mM $MgCl_2$ (final AAC concentration 3.5 µg/mL) and incubated for 2.5 h at 25°C. The obtained solution was used to incubate three silicon chips for 1 h at RT. Chips were then washed 10 min in PBS rinsed with 2 mM $MgCl_2$ and dried. Chips were then incubated with Cy5-labeled antiCD63 and Cy3-labeled antiCD81 (each 1 µg/mL in PBS) for 45 min at RT. Chips were washed 10 min in PBS rinsed with 2 mM $MgCl_2$, dried and finally scanned using ExoView R100.

2.12 Characterization of EVs separated from human Plasma

2.12.1 Transmission Electron Microscopy

1.5 mg of streptavidin coated magnetic beads were functionalized with antiCD9-Tag2 as described in Section 2.5. Beads were then incubated with 600 µL human plasma added with 2 mM $MgCl_2$ for 2.5 h at 25°C under stirring. Beads were then washed twice with 300 µL of PBS-M and incubated with 50 µL of 4 mM biotin in PBS for 1 h at 25°C under stirring. After incubation, the supernatant was recollected and stored at -80°C upon analysis. Trasmission Electron Microscopy (TEM) was performed on supernatant to analyze their ultrastructural morphology. According to proper dilution, the sample was adsorbed to 300 mesh carbon-coated copper grids (Electron Microscopy Sciences, Hatfield, PA, USA) for 5 min in a humid chamber at room temperature. EVs on grids were then fixed in 2% glutaralhdehyde (Electron Microscopy Sciences, Hatfield, PA, USA) in PBS for 10 min and then briefly rinsed in milli-Q water. Grids with adhered EVs were examined with a Philips CM 100 transmission electron microscope at 80 kV, after negative staining with 2% phosphotungstic acid, brough to pH 7.0 with NaOH. The images were captured by a Kodak digital camera.

2.12.2 Western Blot

1.5 mg of streptavidin coated magnetic beads were functionalized with antiCD9-Tag2 as described in Section 2.5. Beads were then incubated with 600 µL human plasma added with 2 mM $MgCl_2$ for 2.5 h at 25°C under stirring. Beads were then washed twice with 300 µL of PBS-M and incubated with 50 µL of 4 mM biotin in PBS for 1 h at 25°C under stirring. After incubation, the supernatant was recollected. A Jess automated Western blot system (Bio-Techne, Minneapolis, MN, USA) was used to measure the expression of CD63 (MAB50482-SP, Human CD63, R&D System), CD81 (MAB46152-SP, Human CD81, R&D System), Flotilin-1 (NBP1-79022, Human Flotilin-1, Novus Biologicals), TSG-101 (NBP2-67884, Human TSG-101, Novus Biologicals) and ApoA1 (GTX112692, Human Apolipoprotein A1, Genetex). Antibodies were diluted 1:10 with antibody diluent 2 and 10 µL were added following manufacturer's instructions.

Briefly, 4 µL of 5X lysis buffer containing β-mercapto ethanol were added to 16ul of eluted sample. Then, 9 µL 0.1X Sample Buffer was added to 19ul of the lysate followed by 7 µL of 5X mastermix. All samples were loaded and analyzed following the manufacturer's instructions using a 12-230-kDa separation module (SM-W004, Bio-Techne, Minneapolis, MN, USA) and the dedicated anti-rabbit secondary antibody (DM-002, Bio-techne, Minneapolis, MN, USA). Chemiluminescence data were analyzed by Compass software (version 6.20, Bio-Techne, Minneapolis, MN, USA).

2.12.3 Nanoparticle Tracking Analysis

Supernatants recovered from magnetic beads were analyzed using Nanosight NS300 (Malvern Panalytical, Malvern, UK). Videos were analyzed by the in-built NanoSight Software NTA 3.2 Dev Build 3.2.16. The Camera type, Camera level, and Detect Threshold were sCMOS, 12 and 5, respectively. The number of completed tracks in NTA measurements was 5 (a 60 seconds movie was registered for each measurement). Sample was diluted in PBS to a final volume of 1 mL. The ideal concentration was assessed by pre-testing the optimal particle per frame value (20-100 particles per frame).

2.13 Multiplexed analysis of EVs separated from human plasma

0.5 mg of streptavidin coated magnetic beads were functionalized with antiCD9-Tag2 as described in Section 2.5. Beads were then incubated with 250 µL human plasma added with 2 mM $MgCl_2$ for 2.5 h at 25°C under stirring. Beads were then washed twice with 250 µL of PBS-M and incubated with 250 µL of 3.5 µg/mL antiCD63-Tag1 in PBS-M for 1 h 25°C under stirring. Beads were then washed twice with 250 µL of PBS-M and incubated with 50 µL of 4 mM biotin in PBS for 1 h at 25°C under stirring. After incubation, the supernatant was recollected. Three silicon chips were coated with MCP-2 and functionalized with Probe1, Probe2 and Probe3 as described is Section 2.4. Supernatant recollected from beads was used to incubate the silicon chips for 1 h at RT. Chips were then washed 10 min in PBS rinsed with 2 mM $MgCl_2$ and dried. Chips were finally scanned using ExoView R100.

3. Results & Discussion

The immunoaffinity separation of extracellular vesicles (EVs), despite having several drawbacks, still exhibits unique features that cannot be matched by other techniques. These include a high degree of selectivity and the ability to target specific subpopulations of EVs. Both of these characteristics are essential for the diagnostic applications of EVs.

To overcome the limitations associated with immunoaffinity separation while retaining its advantages, we propose a novel approach for the simultaneous separation and detection of EVs from biological fluids. The method we suggest utilizes an antibody-aptamer conjugate (AAC).

AAC is a three-component reagent that consists of an antibody linked to a single-stranded DNA (ssDNA) sequence. The ssDNA comprises two distinct regions: a streptavidin binding aptamer and a unique "barcode" sequence.

The assay employing AACs is illustrated in Figure 1: In the initial step, AAC is immobilized on the surface of streptavidin-coated magnetic beads, taking advantage of the aptamer's affinity. Then, the antibody can bind to EVs. Subsequently, once the binding of EVs occurred, the AACs can be detached from the bead surface through incubation with biotin, which displaces the aptamer from streptavidin. After this detachment, the AAC is recaptured on the surface of a DNA microarray chip that has been functionalized with DNA sequences complementary to the barcode region of the AAC.

The use of AAC enables both the separation and detection to be carried out using the same reagent. Furthermore, by pairing antibodies that target various EV surface markers with different barcode sequences, this proposed approach, when combined with a microarray chip for detection, can be utilized for conducting multiplexed analysis of EVs.

To demonstrate that the aptamer sequence, when linked to an antibody, retains its ability to bind to streptavidin, we connected two DNA sequences to a polyclonal rabbit IgG: StrepApt5 (which is the exact aptamer sequence) and StrepApt5-5A (the same sequence with the addition of 5 adenines at the 5' end to act as a spacer between the aptamer and the antibody). These resulting conjugates were used to incubate microarray chips that were printed with various concentrations of streptavidin, ranging from 0.2 to 2 mg/mL. After incubation with a secondary antibody, we analyzed the amount of AAC bound to streptavidin, and the results are presented in Figure 2. Both conjugates could be immobilized on streptavidin, confirming that the aptamer remains effective even after conjugation, and they displayed the same trend with more AAC being immobilized on spots corresponding to higher concentrations of streptavidin.

We evaluated the effectiveness of the biotin-mediated release of the same AACs on different chips, and the results indicate that the conjugates behave similarly. They can both be released from streptavidin upon incubation with 4 mM biotin in PBS, as shown in Figure S1 (see Supporting Information). Given that the inclusion of the 5-adenine spacer yielded slightly better results in terms of reversible immobilization on streptavidin (along with narrower standard deviation values), we decided to incorporate the spacer into the DNA sequences for use in subsequent experiments.

We fused three different and selective barcodes with StrepApt5-5A, resulting in single-stranded DNA sequences named Tag1, Tag2, and Tag3. These sequences were then

conjugated to polyclonal rabbit IgG, producing Rabbit IgG-Tag1, Rabbit IgG-Tag2, and Rabbit IgG-Tag3, respectively.

The resulting conjugates were immobilized on separate series of microarray chips, each of which was functionalized with 2 mg/mL streptavidin as described in Section 2.6. We then assessed aptamer-directed immobilization and biotin-mediated release, and the results are depicted in Figure 3. All the conjugates were successfully immobilized on the surface of streptavidin spots and could be released when challenged by biotin.

To determine whether AACs released from streptavidin could indeed be recaptured on DNA microarrays by exploiting their barcode region, we immobilized the same conjugates on separate aliquots of streptavidin-coated magnetic beads. These conjugates were then released through competition with biotin, and the resulting supernatants were used to incubate silicon microarray chips that had been functionalized with DNA sequences complementary to the barcodes, specifically Probe1, Probe2, and Probe3, as described in Section 2.7.

As shown in Figure 4, the results confirm that AACs can be effectively and reversibly immobilized on streptavidin-coated magnetic beads. After biotin-mediated release, they can be selectively recaptured on the surface of a DNA microarray only in correspondence with the complementary probe.

Having established that the proposed approach works as a proof of concept, we then applied it to samples containing extracellular vesicles (EVs). First, we employed the experimental protocol to EVs that had been separated from the HEK-293 cell culture supernatant through ultracentrifugation. These EVs were diluted to a concentration of $1*10^{10}$ particles/mL in PBS-M and were incubated with streptavidin-coated magnetic beads that had been previously functionalized with antiCD9-Tag2. After the capture of EVs and biotin-mediated release, the supernatant was collected and used to incubate silicon chips that had been functionalized with Probe2 (the probe that binds to the Tag2 barcode), as well as two negative controls (Probe3 and Rabbit IgG). The chips were then scanned using ExoView R100, and the results are presented in Figure 5.

A remarkably strong signal was observed on Probe2, indicating an exceptionally effective binding of EVs to the spot. In contrast, only weak signals were recorded on the negative controls. This outcome validates the use of AACs and the proposed methodology for the separation and analysis of EVs. It also demonstrates that all components of AACs, including the antibody, the aptamer, and the barcode, remain functional even after the conjugation reaction.

Within the same experiment, a portion of the beads was functionalized with antiCD9-Tag2 and then incubated solely with PBS-M as a negative control. These beads were treated with 4 mM biotin, and the resulting supernatant was used to incubate microarray chips. After detection by label-free interferometry, no signal was detected on the spots. This indicates that AAC alone, in the absence of EVs, does not produce a signal on the ExoView R100 instrument.

To demonstrate the applicability of the proposed approach to the separation of EVs from complex biological fluids, a series of experiments starting with human plasma was designed. AntiCD9-Tag2 was immobilized on streptavidin-coated magnetic beads. The beads were then incubated with human plasma to which 2 mM $MgCl_2$ was added, and this incubation lasted for 2.5 hours at 25°C. After thorough washes, the beads were incubated with 4 mM biotin in PBS for 1 hour at 25°C. The resulting supernatant was collected and used to incubate silicon chips that had been functionalized with Probe2, Probe3, and Rabbit IgG, as was done in the previous experiment. After recapturing EVs on the chips, they were incubated with fluorescent secondary antibodies, specifically Cy5-labeled antiCD63 and Cy3-labeled antiCD81. This additional step was carried out to further confirm that the particles registered were indeed EVs and not one of the numerous contaminants typically present in human plasma.

Subsequently, the chips were scanned using the ExoView R100, and the results (refer to Figure 6a) confirm that a substantial number of EVs were captured only on the Probe2 spots, while only weak signals were detected on the negative controls. Interestingly, there is a clear correlation between the label-free measurements and the signals detected by both green and red fluorescence, confirming that the majority of particles detected by the instrument are indeed EVs.

As a negative control, magnetic beads were functionalized with Rabbit IgG-Tag2 and subjected to the same experimental procedure. As illustrated in Figure 6b, a strong signal was detected in the label-free configuration exclusively on Probe2, but there was no correlation with fluorescent signals. This outcome suggests that Rabbit IgG likely interacts with contaminants in plasma that behave like nanoparticles in label-free interferometry, but not with EVs.

Figure 6c demonstrates the results obtained by incubating "naked" beads, which are streptavidin-coated magnetic beads that have not been functionalized with any AAC. This confirms that the presence of AACs on the beads is essential for capturing EVs from plasma.

Finally, Figure 6d reveals particles that were captured and labeled with fluorescence on the

microarray chip after incubation with human plasma to which 2 mM MgCl2 and 3.5 µg/mL antiCD9-Tag2 were added. In this case, a substantial number of particles (both in label-free and fluorescence mode) were detected on all series of spots, not just on Probe2. This result highlights the importance of the initial separation step on magnetic beads in obtaining a clear analysis of EVs contained in the sample, especially when starting with complex fluids such as human plasma.

The experiment involving human plasma was repeated on larger batches, as described in Section 2.12, to conduct the characterization of EVs separated using AACs (refer to Figure 7). After the incubation of magnetic beads with biotin, the supernatant was collected and subjected to analysis using Transmission Electron Microscopy (TEM), Nanoparticle Tracking Analysis (NTA), and Western Blot.

NTA revealed the presence of nanoparticles in the supernatant, ranging in size from 100 to 300 nm, which is consistent with an EV population. This finding was corroborated by TEM measurements, which highlighted the presence of intact nanovesicles enclosed within a lipid membrane.

Western Blot analysis confirmed the presence of both surface and luminal EV markers (CD63, CD81, Flotilin-1, and TSG101). Apolipoprotein A1 was detected as a contaminant at this stage. However, previous results involving human plasma (as seen in Figure 6a) suggest that the secondary discrimination introduced by the DNA microarray chip might be adequate to remove the majority of these contaminants, especially those that are prevalent in biological fluids.

To provide a proof of concept that the separation of EVs and their multiplexed analysis on a DNA microarray can be achieved using AACs, we designed an additional experiment. We functionalized streptavidin-coated magnetic beads with antiCD9-Tag2 and incubated them with human plasma to which 2 mM MgCl2 was added. After washing the beads, we incubated them with antiCD63-Tag1 to label the EVs captured on the beads. Subsequently, the beads were incubated with biotin, and the resulting supernatant was collected and used to incubate microarray chips that had been functionalized with Probe1, Probe2 and Probe3. These chips were then analyzed using label-free interferometry.

The results, as depicted in Figure 8, confirm that both CD9+ and CD63+ EVs were recaptured on Probe2 and Probe1, respectively, while only weak signals were detected on Probe3, which serves as the negative control. The signal measured for CD9+ EVs was higher than that of CD63+ particles. It should be noted that, as EV capture was carried out

using the aCD9-Tag2 antibody, the results indicate the co-expression of CD63 on CD9+ EVs in the sample.

4. Conclusion

We have developed a three component reagent that allows the consequential separation and analysis of EVs from complex biological fluids. This reagent consists of a DNA-antibody conjugate, wherein the DNA sequence comprises two sections: an aptamer that binds to streptavidin and a barcode region. The conjugate can be immobilized onto the surface of streptavidin-coated magnetic beads, making use of the aptamer's affinity, and in a subsequent step, it can be detached from the beads by employing biotin. Likewise, it can be recaptured on the surface of a DNA microarray decorated with oligonucleotide sequences that complement the barcode regions.

Our reagent has demonstrated its effectiveness in separating EVs from human plasma and allowing their detection through label-free interferometry. We believe that this approach represents a significant advancement in the field of immunoaffinity separation and analysis of EVs and holds the potential to open pathways for diagnostic applications involving EV detection.

5. Acknowledgements

This research was funded by European Commission through the HORIZON-EIC-2021-TRANSITIONOPEN-01 project NEXUS (automated in-line separatioN and dEtection of eXtracellular vesicles for liqUid biopsy applicationS) under Grant Number 101058200.

The authors are grateful to Dr. R. Vago (Urological Research Institute, Division of Experimental Oncology, IRCCS San Raffaele Scientific Institute, Milan, Italy) for providing HEK-derived EV samples, and to Dr. Y. D'Alessandra (Bio-Techne) for performing Western Blot analyses.

6. Appendix A. Supporting information

7. Conflicts of interest

M. Chiari, D. Brambilla and M. S. Ünlü have filed the US Provisional Appl. No. 63/383,930 entitled “METHODS AND COMPOSITION RELATING TO PARTICLE CAPTURE”.

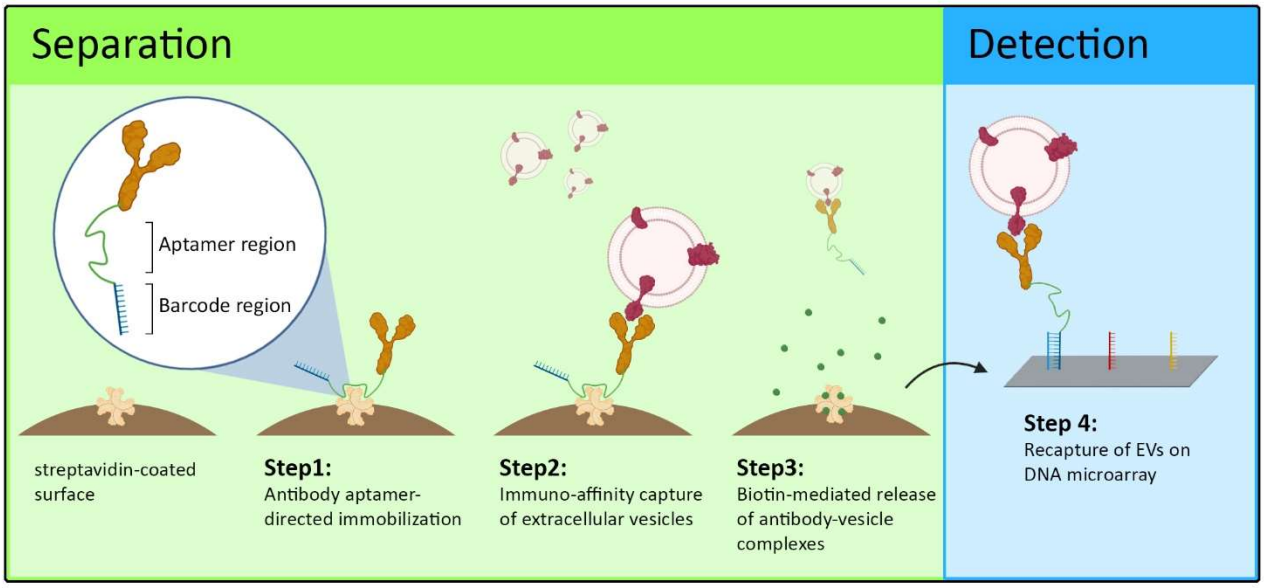

Figure 1. *Representation of concomitant separation and detection of EVs using AACs.*

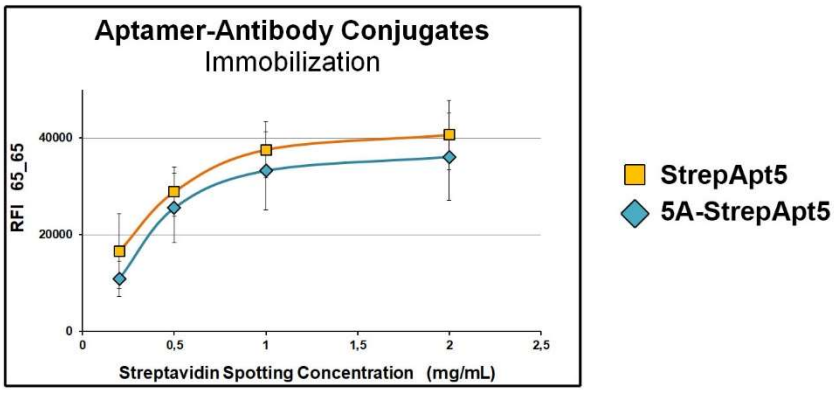

Figure 2. *Amount of AACs (Rabbit IgG-StrepApt5 and Rabbit IgG-StrepApt5-5A) immobilized on different concentrations of streptavidin printed on a microarray chip.*

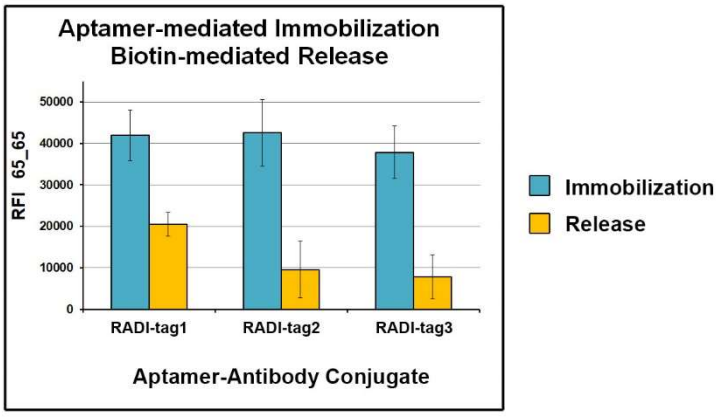

***Figure 3**. Amount of different AACs (Rabbit IgG-Tag1, Rabbit IgG-Tag2 and Rabbit IgG-Tag3) immobilized on 2 mg/mL streptavidin and released after incubation with biotin.*

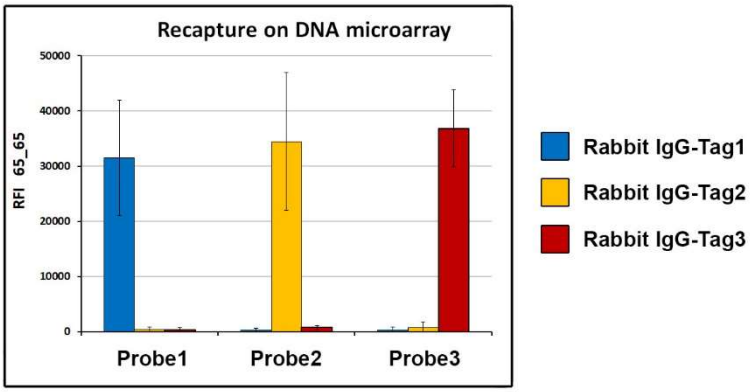

***Figure 4**. Sequence-selective recapture on DNA microarray of 3 different AACs previously immobilized on streptavidin coated magnetic beads and released upon incubation with biotin.*

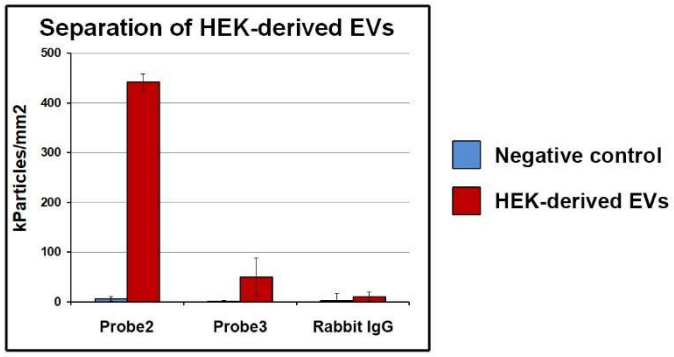

***Figure 5**. Detection of EVs by label free interferometry separated and recaptured on DNA microarray using antiCD9-Tag2 (red bars). In the negative control, AAC-functionalized magnetic beads were incubated only with PBS-M (blue bars).*

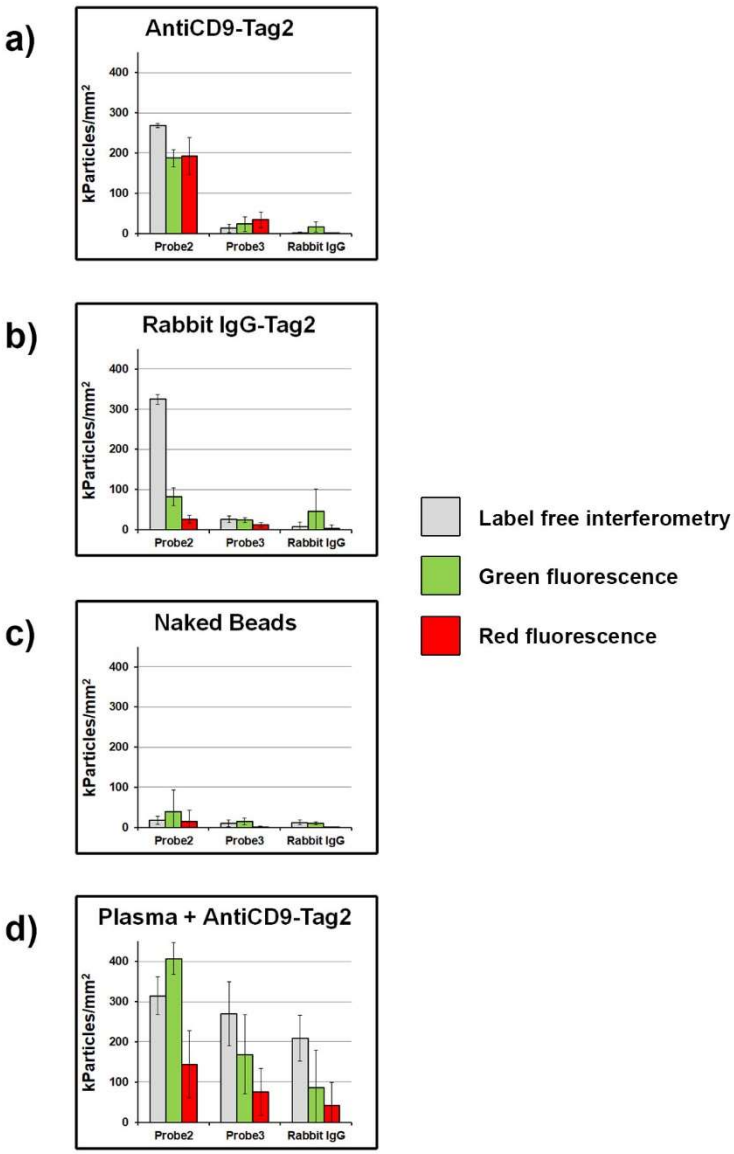

***Figure 6**. Label free interferometric and fluorescent detection of EVs on DNA microarray after separation using streptavidin coated magnetic beads: (a) functionalized with antiCD9-Tag2; (b) functionalized with Rabbit IgG-Tag2; (c) non functionalized with AACs. As additional negative control, detection of plasma added with antiCD9-Tag2 without previous separation of EVs on magnetic beads (d).*

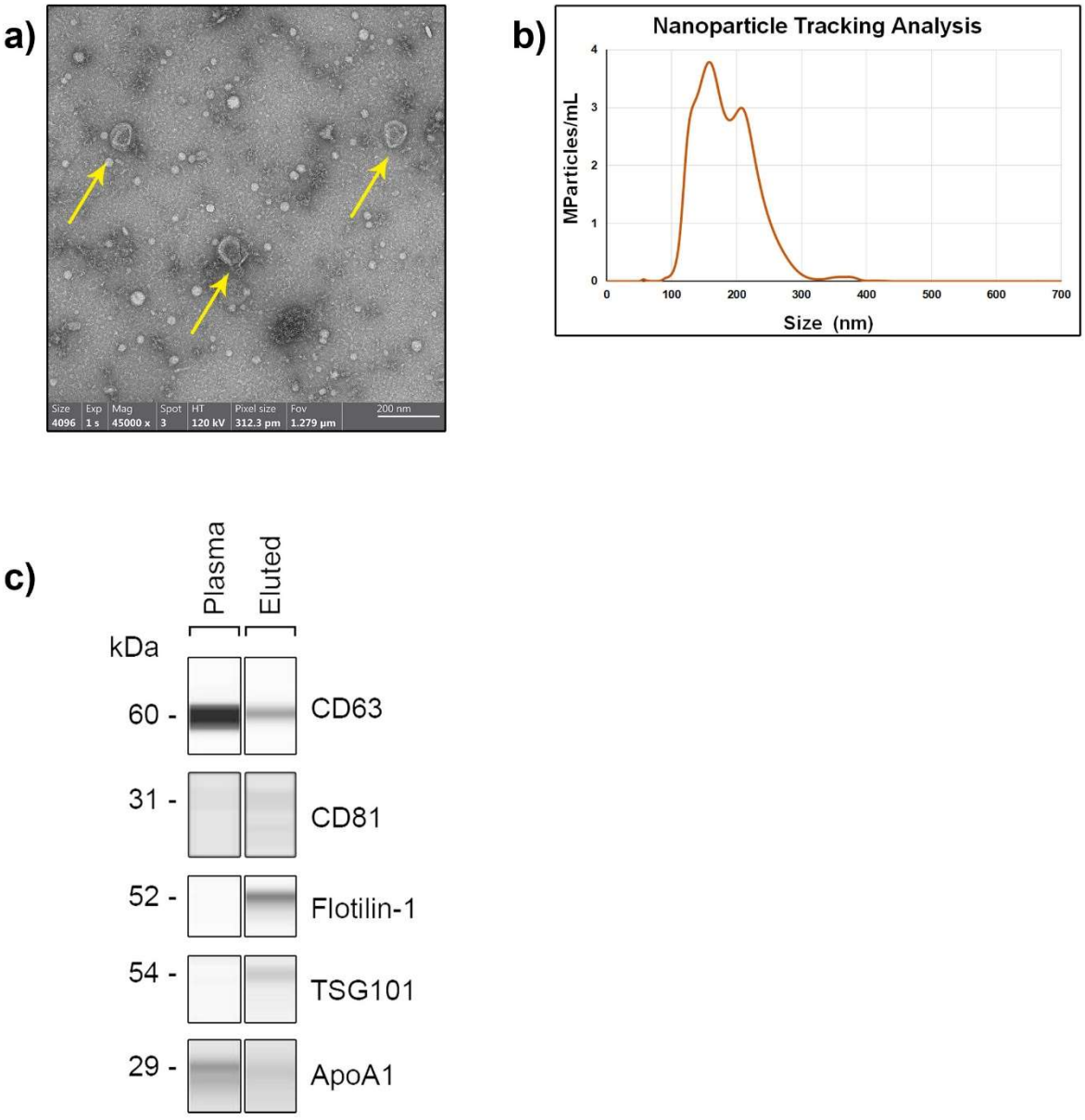

***Figure 7**. Analysis of EVs separated using antiCD9-Tag2 functionalized magnetic beads by: (a) Transmission Electron Microscopy; (b) Nanoparticle Tracking Analysis; (c) Western Blot.*

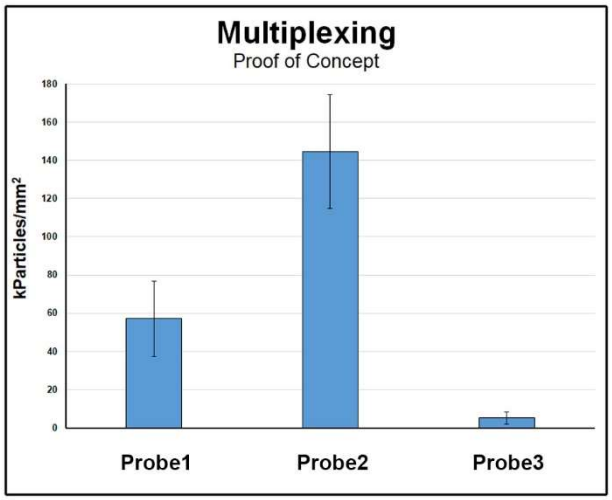

***Figure 8**. Recapture and multiplexed detection on DNA microarray of EVs separated using antiCD9-Tag2 immobilized on magnetic beads and labeled using antiCD63-Tag1.*

5. References

[1] C. Théry, K.W. Witwer, E. Aikawa, M. Jose Alcaraz, J.D. Anderson, R. Andriantsitohaina, A. Antoniou, M. Bach, D. Bachurski, H. Baharvand, L. Balaj, S. Baldacchino, N.N. Bauer, A.A. Baxter, M. Bebawy, C. Beckham, A. Bedina Zavec, A. Benmoussa, A.C. Berardi, P. Bergese, E. Bielska, C. Blenkiron, S. Bobis-Wozowicz, E. Boilard, W. Boireau, A. Bongiovanni, F.E. Borràs, S. Bosch, C.M. Boulanger, X. Breakefield, A.M. Breglio, M. Á Brennan, D.R. Brigstock, A. Brisson, M.L. Broekman, J.F. Bromberg, P. Bryl-Górecka, S. Buch, A.H. Buck, D. Burger, S. Busatto, D. Buschmann, B. Bussolati, E.I. Buzás, J. Bryan Byrd, G. Camussi, D.R. Carter, S. Caruso, L.W. Chamley, Y.-T. Chang, C. Chen, S. Chen, L. Cheng, A.R. Chin, A. Clayton, S.P. Clerici, A. Cocks, E. Cocucci, R.J. Coffey, A. Cordeiro-da-Silva, Y. Couch, F.A. Coumans, B. Coyle, R. Crescitelli, M. Ferreira Criado, S. Das, A. Datta Chaudhuri, P. de Candia, E.F. De Santana Junior, O. De Wever, H.A. del Portillo, T. Demaret, S. Deville, A. Devitt, B. Dhondt, D. Di Vizio, L.C. Dieterich, V. Dolo, A. Paula Dominguez Rubio, M. Dominici, M.R. Dourado, T.A. Driedonks, F. V Duarte, H.M. Duncan, R.M. Eichenberger, K. Ekström, S. EL Andaloussi, C. Elie-Caille, U. Erdbrügger, J.M. Falcón-Pérez, F. Fatima, J.E. Fish, M. Flores-Bellver, A. Försönits, A. Frelet-Barrand, F. Fricke, G. Fuhrmann, S. Gabrielsson, A. Gámez-Valero, C. Gardiner, K. Gärtner, R. Gaudin, Y. Song Gho, B. Giebel, C. Gilbert, M. Gimona, I. Giusti, D.C. Goberdhan, A. Görgens, S.M. Gorski, D.W. Greening, J. Christina

Gross, A. Gualerzi, G.N. Gupta, D. Gustafson, A. Handberg, R.A. Haraszti, P. Harrison, H. Hegyesi, A. Hendrix, A.F. Hill, F.H. Hochberg, K.F. Hoffmann, B. Holder, H. Holthofer, B. Hosseinkhani, G. Hu, Y. Huang, V. Huber, S. Hunt, A. Gamal-Eldin Ibrahim, T. Ikezu, J.M. Inal, M. Isin, A. Ivanova, H.K. Jackson, S. Jacobsen, S.M. Jay, M. Jayachandran, G. Jenster, L. Jiang, S.M. Johnson, J.C. Jones, A. Jong, T. Jovanovic-Talisman, S. Jung, Journal of Extracellular Vesicles Minimal information for studies of extracellular vesicles 2018 (MISEV2018): a position statement of the International Society for Extracellular Vesicles and update of the MISEV2014 guidelines, (n.d.). https://www.tandfonline.com/loi/zjev20 (accessed January 24, 2020).

[2] M.P. Zaborowski, L. Balaj, X.O. Breakefield, C.P. Lai, Extracellular Vesicles: Composition, Biological Relevance, and Methods of Study, Bioscience. 65 (2015). https://doi.org/10.1093/biosci/biv084.

[3] B. Pang, Y. Zhu, J. Ni, J. Thompson, D. Malouf, J. Bucci, P. Graham, Y. Li, Extracellular vesicles: the next generation of biomarkers for liquid biopsy-based prostate cancer diagnosis, Theranostics. 10 (2020) 2309–2326. https://doi.org/10.7150/thno.39486.

[4] J. Liu, Y. Chen, F. Pei, C. Zeng, Y. Yao, W. Liao, Z. Zhao, Review Article Extracellular Vesicles in Liquid Biopsies: Potential for Disease Diagnosis, (2021). https://doi.org/10.1155/2021/6611244.

[5] C. Théry, S. Amigorena, G. Raposo, A. Clayton, Isolation and Characterization of Exosomes from Cell Culture Supernatants and Biological Fluids, Curr. Protoc. Cell Biol. 30 (2006) 3.22.1-3.22.29. https://doi.org/10.1002/0471143030.cb0322s30.

[6] B.J. Tauro, D.W. Greening, R.A. Mathias, H. Ji, S. Mathivanan, A.M. Scott, R.J. Simpson, Comparison of ultracentrifugation, density gradient separation, and immunoaffinity capture methods for isolating human colon cancer cell line LIM1863-derived exosomes, Methods. 56 (2012) 293–304. https://doi.org/10.1016/j.ymeth.2012.01.002.

[7] J.Z. Nordin, Y. Lee, P. Vader, I. Mäger, H.J. Johansson, W. Heusermann, O.P.B. Wiklander, M. Hällbrink, Y. Seow, J.J. Bultema, J. Gilthorpe, T. Davies, P.J. Fairchild, S. Gabrielsson, N.C. Meisner-Kober, J. Lehtiö, C.I.E. Smith, M.J.A. Wood, S. EL Andaloussi, Ultrafiltration with size-exclusion liquid chromatography for high yield isolation of extracellular vesicles preserving intact biophysical and functional properties, Nanomedicine Nanotechnology, Biol. Med. 11 (2015) 879–883.

https://doi.org/10.1016/j.nano.2015.01.003.

[8] A.N. Böing, E. van der Pol, A.E. Grootemaat, F.A.W. Coumans, A. Sturk, R. Nieuwland, Single-step isolation of extracellular vesicles by size-exclusion chromatography., J. Extracell. Vesicles. 3 (2014). https://doi.org/10.3402/jev.v3.23430.

[9] K.R. Yamamoto, B.M. Alberts, R. Benzinger, L. Lawhorne, G. Treiber, Rapid bacteriophage sedimentation in the presence of polyethylene glycol and its application to large-scale virus purification, Virology. 40 (1970) 734–744. https://doi.org/10.1016/0042-6822(70)90218-7.

[10] A. Adams, Concentration of Epstein-Barr Virus from Cell Culture Fluids with Polyethylene Glycol, J. Gen. Virol. 20 (1973) 391–394. https://doi.org/10.1099/0022-1317-20-3-391.

[11] A. Ghosh, M. Davey, I.C. Chute, S.G. Griffiths, S. Lewis, S. Chacko, D. Barnett, N. Crapoulet, S. Fournier, A. Joy, M.C. Caissie, A.D. Ferguson, M. Daigle, M.V. Meli, S.M. Lewis, R.J. Ouellette, Rapid Isolation of Extracellular Vesicles from Cell Culture and Biological Fluids Using a Synthetic Peptide with Specific Affinity for Heat Shock Proteins, PLoS One. 9 (2014) e110443. https://doi.org/10.1371/JOURNAL.PONE.0110443.

[12] K. Wang, S. Zhang, J. Weber, D. Baxter, D.J. Galas, Export of microRNAs and microRNA-protective protein by mammalian cells, Nucleic Acids Res. 38 (2010) 7248–7259. https://doi.org/10.1093/nar/gkq601.

[13] K. Kluszczyńska, L. Czernek, W. Cypryk, Ł. Pęczek, M. Düchler, Methods for the Determination of the Purity of Exosomes, Curr. Pharm. Des. 25 (2019) 4464–4485. https://doi.org/10.2174/1381612825666191206162712.

[14] M.Y. Konoshenko, E.A. Lekchnov, A. V. Vlassov, P.P. Laktionov, Isolation of Extracellular Vesicles: General Methodologies and Latest Trends, Biomed Res. Int. 2018 (2018). https://doi.org/10.1155/2018/8545347.

[15] D. Brambilla, L. Sola, A.M. Ferretti, E. Chiodi, N. Zarovni, D. Fortunato, M. Criscuoli, V. Dolo, I. Giusti, V. Murdica, K. Kluszczyńska, L. Czernek, M. Düchler, R. Vago, M. Chiari, EV Separation: Release of Intact Extracellular Vesicles Immunocaptured on Magnetic Particles, Anal. Chem. 93 (2021) 5476–5483. https://doi.org/10.1021/ACS.ANALCHEM.0C05194.

[16] H. Zhang, Q. Zhang, Y. Deng, M. Chen, C. Yang, Improving Isolation of Extracellular Vesicles by Utilizing Nanomaterials, Membr. 2022, Vol. 12, Page 55. 12 (2021) 55.

https://doi.org/10.3390/MEMBRANES12010055.

[17] K. Zhang, Y. Yue, S. Wu, W. Liu, J. Shi, Z. Zhang, Rapid Capture and Nondestructive Release of Extracellular Vesicles Using Aptamer-Based Magnetic Isolation, ACS Sensors. 4 (2019) 1245–1251. https://doi.org/10.1021/acssensors.9b00060.

[18] V.J.B. Ruigrok, E. van Duijn, A. Barendregt, K. Dyer, J.A. Tainer, R. Stoltenburg, B. Strehlitz, M. Levisson, H. Smidt, J. van der Oost, Kinetic and Stoichiometric Characterisation of Streptavidin-Binding Aptamers, ChemBioChem. 13 (2012) 829–836. https://doi.org/10.1002/cbic.201100774.

[19] D. Brambilla, L. Sola, M. Chiari, Advantageous antibody microarray fabrication through DNA-directed immobilization: A step toward use of extracellular vesicles in diagnostics, Talanta. 222 (2021) 121542. https://doi.org/10.1016/j.talanta.2020.121542.